Carderock Division, Naval Surface Warfare Center

Bethesda, Maryland 20084-5000

CARDIVNSWC-TR-94/024 December 1994

Signatures Directorate

Research and Development Report

Nonlinear Calibration of an Infrared Radiometer

by

Peter O. Cervenka

Carderock Division, Naval Surface Warfare Center

and

Lou Massa

City University of New York

Presented at

Workshop on Infrared Ship Signature Modeling (IRSSM),

organized by the NATO Research Study Group on

Maritime Infrared Target and Background Signatures,

Measurements and Characterization (RSG.5)

17 -18 October 1994

Paris, France

REPORT DOCUMENTATION PAGE

1a. REPORT SECURITY CLASSIFICATION UNCLASSIFIED	1b. RESTRICTIVE MARKINGS
2a. SECURITY CLASSIFICATION AUTHORITY	3. DISTRIBUTION/AVAILABILITY OFREPORT Approved for public release; distribution is unlimited.
2b. DECLASSIFICATION/DOWNGRADING SCHEDULE	
4. PERFORMING ORGANIZATION REPORT NUMBER(S) CARDIVNSWC-TR-94/024	5. MONITORING ORGANIZATION REPORT NUMBER(S)
6a. NAME OF PERFORMING ORGANIZATION Carderock Division Naval Surface Warfare Center 6b. OFFICE SYMBOL (If applicable) Code 7230	7a. NAME OF MONITORING ORGANIZATION
6c. ADDRESS (City, State, and ZIP Code) Bethesda, MD 20084-5000	7b. ADDRESS (CITY, STATE, AND ZIP CODE)
8a. NAME OF FUNDING/SPONSORING ORGANIZATION 6b. OFFICE SYMBOL (If applicable)	9. PROCUREMENT INSTRUMENT IDENTIFICATION NUMBER
8c. ADDRESS (City, State, and ZIP code)	10. SOURCE OF FUNDING NUMBERS PROGRAM ELEMENT NO. 0602121N; PROJECT NO. RH21C17; TASK NO. 3; WORK UNIT ACCESSION NO.

11. TITLE (Include Security Classification)
Nonlinear Calibration of an Infrared Radiometer

12. PERSONAL AUTHOR(S)
Cervenka, Peter O. and Massa, Lou

13a. TYPE OF REPORT	13b. TIME COVERED	14. DATE OF REPORT (Year, Month, Day)	15. PAGE COUNT
Final	FROM: TO:	1994, December	33

16. SUPPLEMENTARY NOTATION Presented at the Workshop on Infrared Ship Signature Modeling (IRSSM), organized by the NATO Research Study Group on Maritime Infrared Target and Background Signatures, Measurements (see reverse side)

17. COSATI CODES			18. SUBJECT TERMS (Continue on reverse if necessary and identity by block number)
FIELD	GROUP	SUB-GROUP	Dimensionless Variables, Infrared Engineering, Infrared Scaling Laws, Scale Model Testing, Thermal Physics

19. ABSTRACT (Continue on reverse if necessary and identify by block number)

At best, the calibration of an infrared radiometer, also known as a Forward Looking Infrared (FLIR) system, is a complex procedure. Effective calibration must (1) be tailored to the actual radiometer being studied, (2) be carried out to each of the many subsystems involved, (3) relate internal system parameters to physical quantities familiar to the infrared community, and (4) be revisited at some interval to ensure that it is still valid. The details of some of the ideas that form the basis for a valid calibration of the GEC Avionics Ltd Dual Waveband Imaging Radiometer FLIR are discussed. The need for the removal of a systematic error due to magnification optics emission, as described by Braim, is emphasized. Another systematic error, associated with an analysis of FLIR gray scale response based upon linear interpolation from reference temperatures, is examined. A novel method of nonlinear interpolation is presented that is aimed at the reduction or elimination of systematic calibration errors.

20. DISTRIBUTION/AVAILABILITY OFABSTRACT	21. ABSTRACT SECURITY CLASSIFICATION	
☒ UNCLASSIFIED/UNLIMITED ☐ SAME AS RPT. ☐ DTIC USERS	UNCLASSIFIED	
22a. NAME OF RESPONSIBLE INDIVIDUAL Peter O. Cervenka	22b. TELEPHONE (Include Area Code) (301) 227-1903	22c. OFFICE SYMBOL Code 7230

DD FORM 1473, 84 MAR

Block 16 (Continued)

and Characterization (RSG.5), 17 - 18 October, 1994, in Paris, France.

CONTENTS

FIGURES

THIS PAGE INTENTIONALLY LEFT BLANK

ABSTRACT

At best, the calibration of an infrared radiometer, also known as a Forward Looking Infrared (FLIR) system, is a complex procedure. Effective calibration must (1) be tailored to the actual radiometer being studied, (2) be carried out for each of the many subsystems involved, (3) relate internal system parameters to physical quantities familiar to the infrared community, and (4) be revisited at some interval to ensure that it is still valid. The details of some of the ideas that form the basis for a valid calibration of the GEC Avionics Ltd Dual Waveband Imaging Radiometer (DUWIR) FLIR are discussed. The need for the removal of a systematic error due to magnification optics emission, as described by Braim, is emphasized. Another systematic error, associated with an analysis of FLIR gray scale response based upon linear interpolation from reference temperatures, is examined. A novel method of nonlinear interpolation is presented that is aimed at the reduction or elimination of systematic calibration errors.

ADMINISTRATIVE INFORMATION

This work is in partial fulfillment of Milestone 2, Task 3, of the Topside Signature Reduction Project (RH21C17) of the Surface Ship Technology Program (SC1A/PE0602121N). The work described herein was sponsored by the Office of the Chief of Naval Research (OCNR 33) and was performed by the Carderock Division, Naval Surface Warfare Center (CDNSWC, Code 7230).

INTRODUCTION

The interest in the FLIR (Forward Looking Infrared) as an imaging radiometer is focused in this report on its use in measuring the infrared contrast between a ship and its background. Unless a FLIR is calibrated, the results obtained will be only of a qualitative value. "*The hundreds if not thousands of next to useless uncalibrated videotapes held across the world containing valuable trials information whose data is in effect irreducible bear witness to this.*"[1] Calibration of the FLIR is therefore of crucial importance in an IR ship measurements program.

CALIBRATION OF GEC DUWIR FLIR

With any calibration, the objective is to obtain a correlation of measured values, y, with true (standard) values, x. Typically, such a correlation is represented by a "calibration curve" such as that shown in Fig. 1. The possibility of calibration is based upon comparison to a trusted standard. Confidence in a calibration is limited by that of the accessible standard.

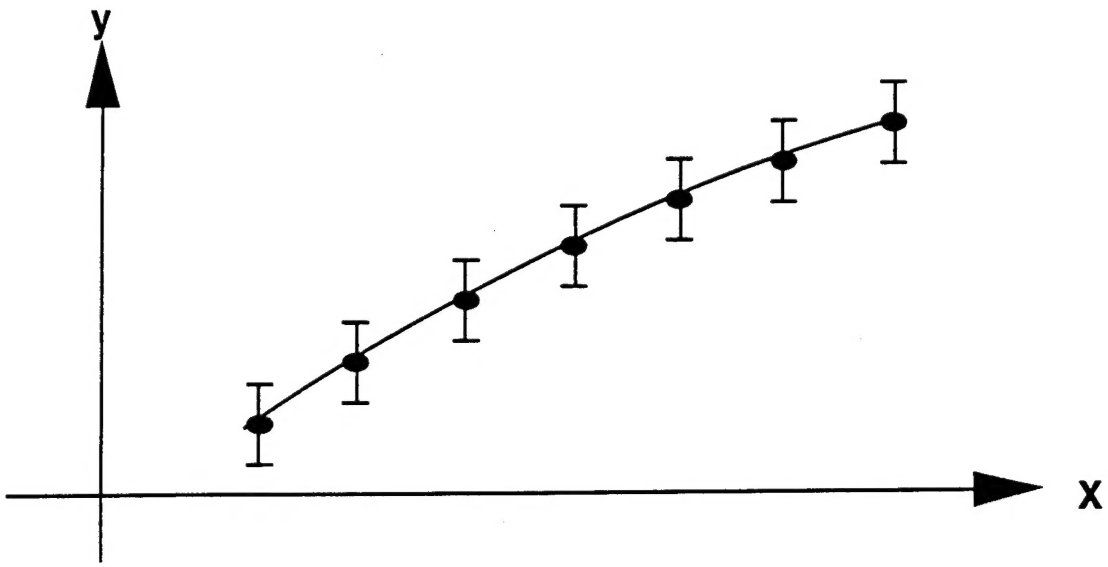

Fig. 1. Typical calibration curve correlating measured values, y, to standard values, x.

Measurements in general and calibrations in particular may contain systematic and random errors. As far as possible, calibration strives to eliminate systematic errors and to place an upper boundary on random errors. Systematic errors (sometimes due to instrument deficiency) and random errors (for instance due to variable fluctuations) affect measurement accuracy and precision, respectively. Accuracy is measured by the "distance" between a test estimate of a physical variable, such as the average, and its standard value; see Fig. 2.

One purpose of calibration is to provide an understanding of the physical sources of measurement errors. For this, it is required to create a theory that encompasses both the variable measured as well as the instrumentation being used. If at all possible, the aim is to reduce both error types and to estimate the magnitudes of the errors that remain. Such understanding can then form the basis for an effective use of the measured data and for subsequent improvement in the calibration.

Unfortunately, calibrations are never concluded once and for all. Instrument characteristics are altered by time and use, and calibration must be viewed as an iterative process as long as an instrument is in use. It is good practice for a measurement laboratory to maintain reliable standards against which periodic recalibration may be performed.

FLIR DESCRIPTION

The Carderock Division of the Naval Surface Warfare Center in Bethesda, Maryland, operates a Dual Waveband Imaging Radiometer (DUWIR) manufactured in the United Kingdom by GEC Avionics Ltd. The following analysis is applicable to the DUWIR system.

The measurement produced by a FLIR is a thermal map of an infrared radiation source and its surroundings. Calibration will affect the entire image produced by a radiometer. Figure 3 shows such a thermal scene in the 8- to 12-μm infrared band (LWIR), which represents a naval vessel at sea on a sunny day.

During the measurement process, imagery is first recorded as analog video on magnetic tape. Figure 4 shows that the FLIR system also contains image analysis hardware that allows the capture in digital format of any single image frame. A typical single frame of FLIR data in digital format is shown in Fig. 5. The image is built up from a rectangular array of pixels. The signal voltage from the FLIR for each pixel is represented by an 8-bit number capable of being represented on a gray scale G of 256 discrete levels. The intensity or gray scale level of each pixel may be examined individually, and associated with a temperature and/or radiance value for that particular pixel. Other data include two reference internal temperatures, displayed in Fig. 5 as Pelt. 1 and Pelt. 2, as well as a scanner internal temperature. In addition, the width of the temperature window W and the offset O which sets the temperature level are also output. These and other data are displayed around the FLIR image in Figs. 6 and 7.

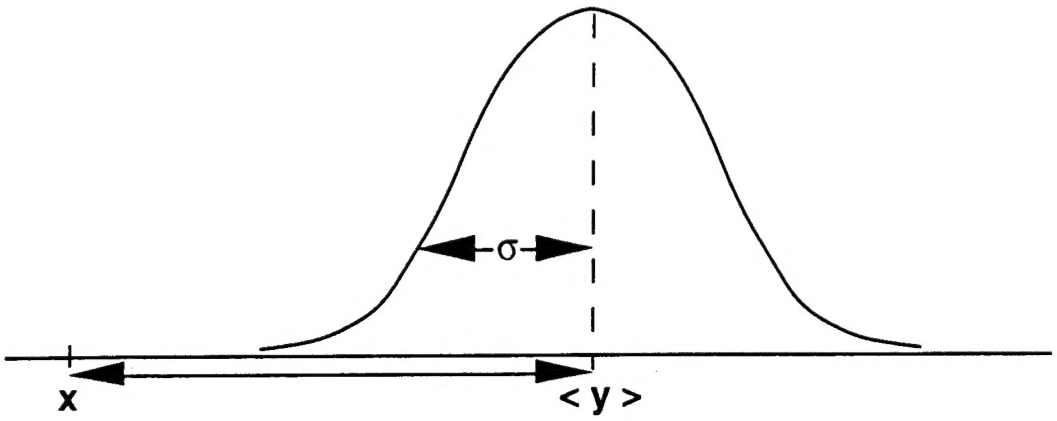

Fig. 2. Measurement accuracy and precision.

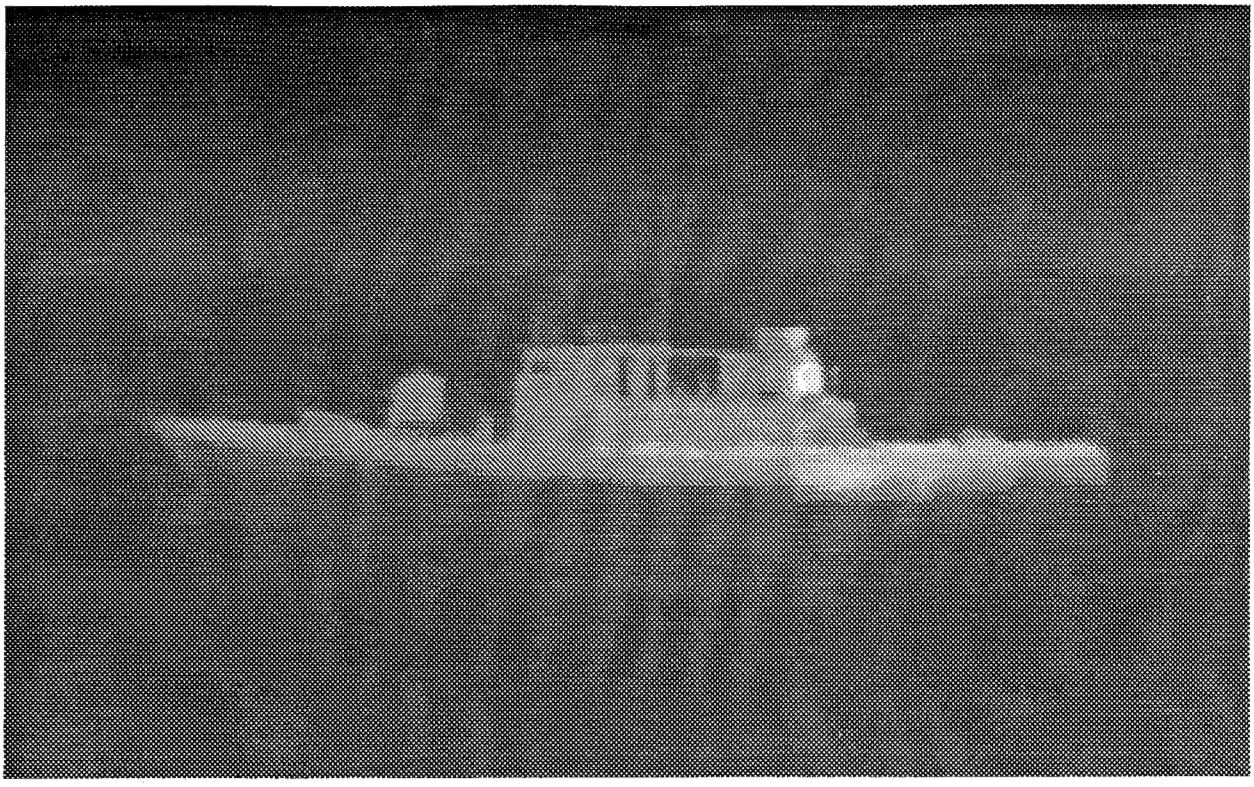

Fig. 3. FLIR image of a naval vessel at sea.

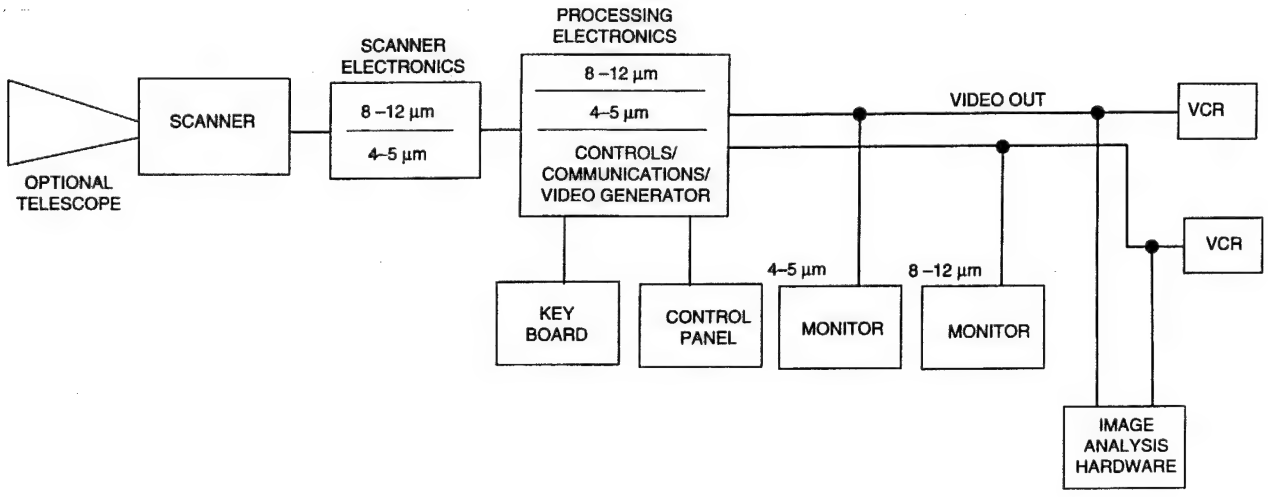

Fig. 4. FLIR system block diagram.

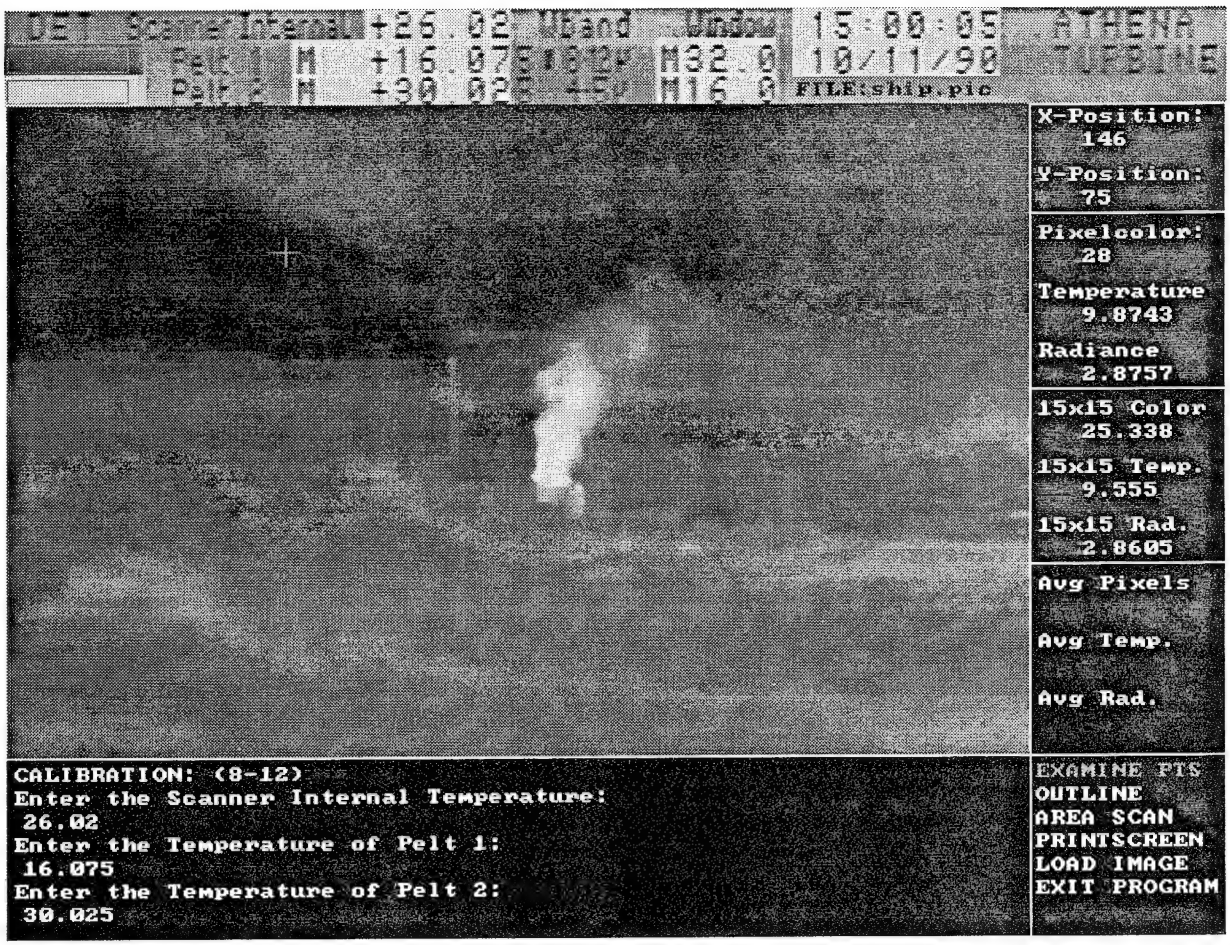

Fig. 5. Single frame of digital FLIR data.

The GEC Avionics Ltd FLIR uses an infrared detector (Fig. 8) that includes two SPRITE (Signal Processing Right in the Element) components respectively sensitive in the 4- to 5-μm and 8- to 12-μm wavebands. The detector material for both wavebands is mercury cadmium telluride.

The FLIR operational scheme is shown in Fig. 9. A study of this block diagram is especially useful in understanding FLIR calibration. Note that the image radiation and optical path are identical for both wavebands from target to detector. Beyond the detector, separate electronic amplification and signal processing serve to record and display the images in each waveband. Note also that two Peltier blackbody reference surfaces are viewed at the edges of each image frame. Platinum, Pt, resistance devices measure the temperatures, T_1 and T_2, of the reference surfaces. Not shown in the figure is a Pt resistance derivative which monitors the temperature, T_s, of the FLIR scanning components. All of these temperatures displayed in Figs. 3 and 7 through 9 are involved in the FLIR calibration. In fact, FLIR calibration minimally involves the measurement variables G_{mn}, T_1, T_2, and T_s; that is, the gray scale response of the pixel (m and n) for all m and n, the temperatures of reference surfaces 1 and 2, and the temperature of the FLIR scanner. As indicated in Fig. 5, each pixel gray scale response G_{mn} is to be associated with a temperature, T_{mn}. It is possible to consider that the basic variable of the FLIR calibration is the temperature or, more specifically, several temperatures, T_{mn} for all (m and n), T_1, T_2, and T_s. The goal in these measurements is to eliminate systematic errors and to quantify random errors.

Obtaining three of the quantities, T_1, T_2, and T_s, is fairly straightforward since the procedure in each case involves a contact measurement of temperature. The calibration simply requires correlation with a known standard, such as a standard thermocouple put into contact and thermal equilibrium with the same thermal mass as the one being measured. In the case of T_1 and T_2, the thermal mass is that of the internal reference surfaces in the FLIR; and in the case of T_s, that of the FLIR scanner assembly. In each of these cases the calibration is a simple procedure, resulting in a single calibration curve for each of the three temperature measurements, similar to that shown in Fig. 1.

The temperature of the two internal reference surfaces, T_1 and T_2, should be calibrated in two different ways. One measurement is a contact measurement which gives the equilibrium temperature of the bulk mass of the internal reference. It is this measurement that would be calibrated against a standard thermocouple attached to the same thermal mass. Another measurement incorporates the gray scale response of the FLIR viewing an external radiating standard blackbody of known temperature. The gray scale response of the FLIR to the external standard is matched against that of the internal reference to obtain a surface temperature of the internal reference. This surface temperature calibration is more complex than the surface contact measurement.

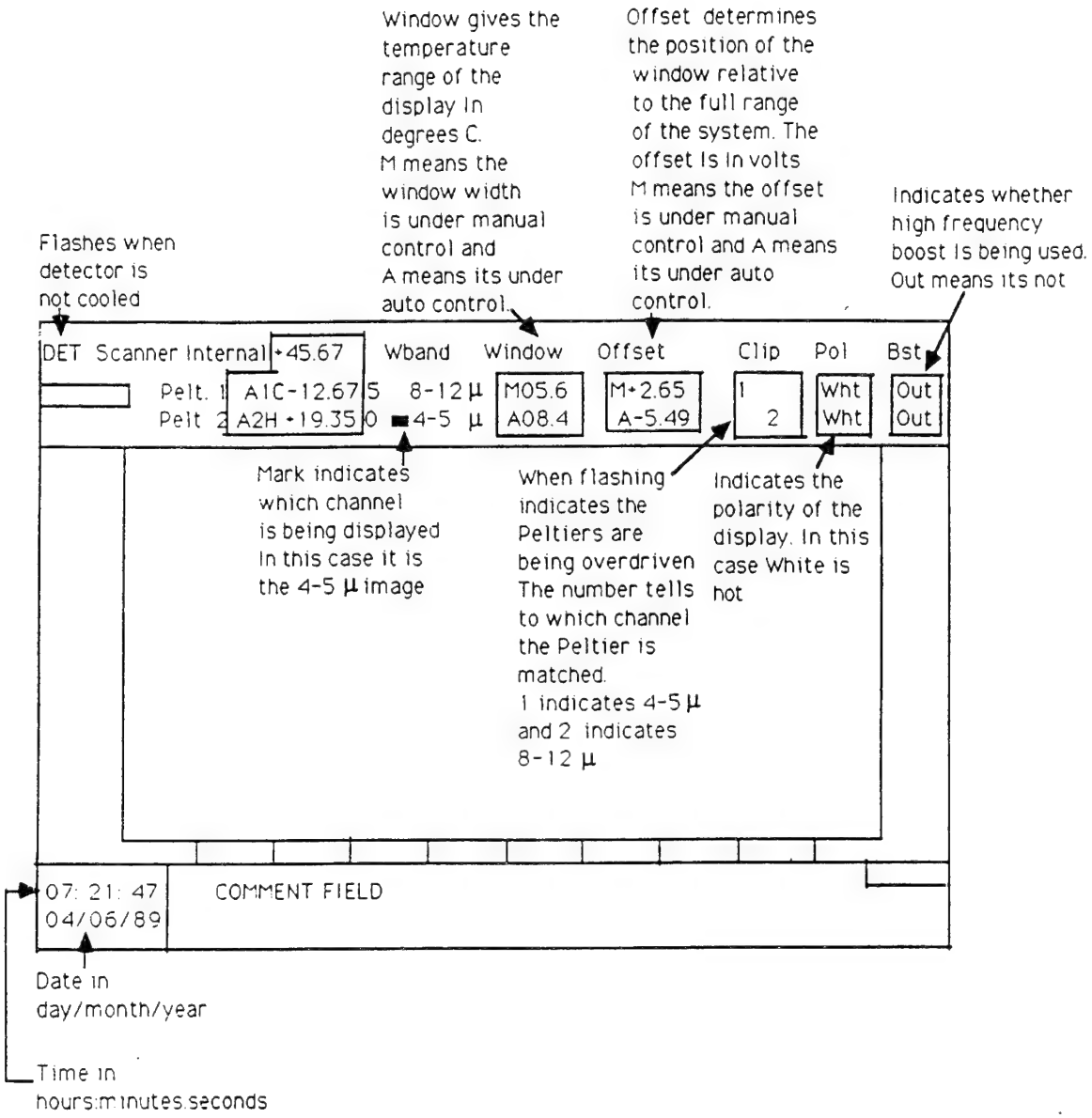

Fig. 6. FLIR display.

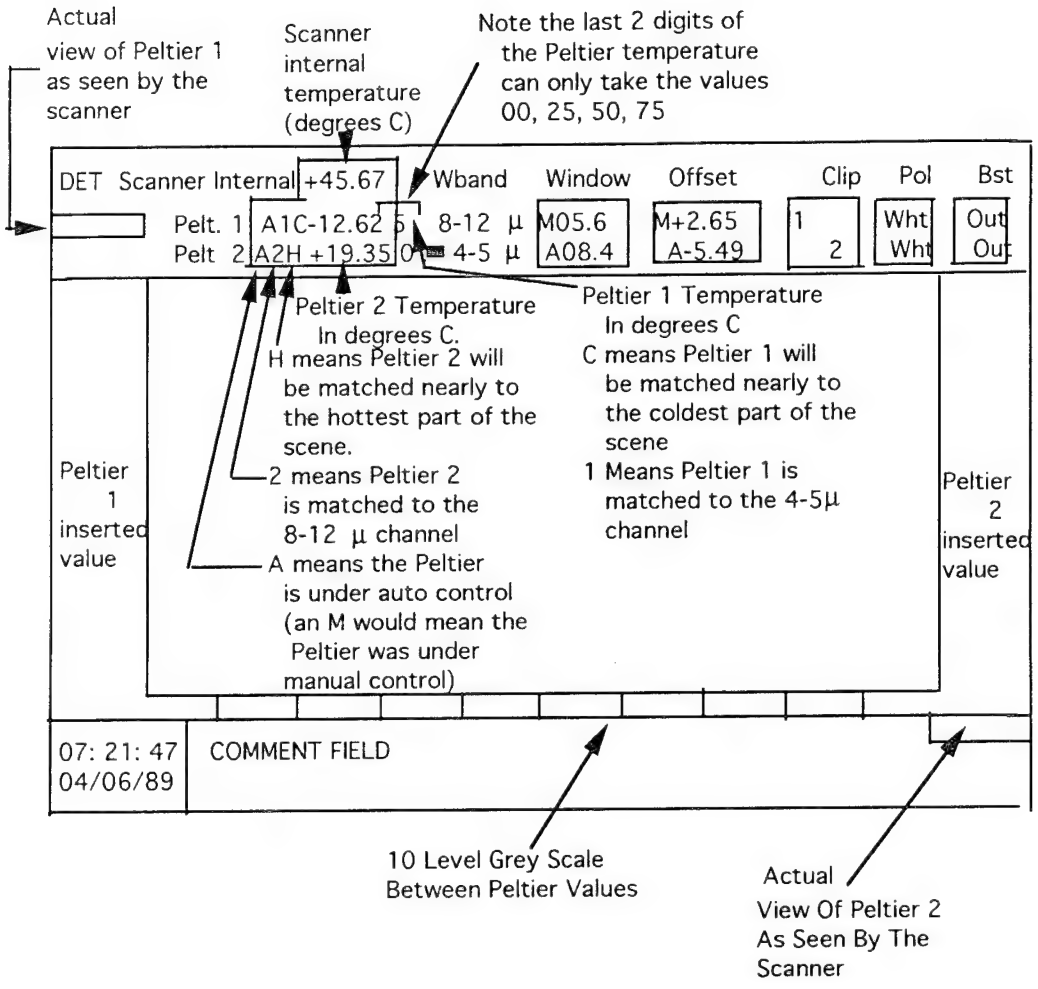

Fig. 7. FLIR display of temperature data.

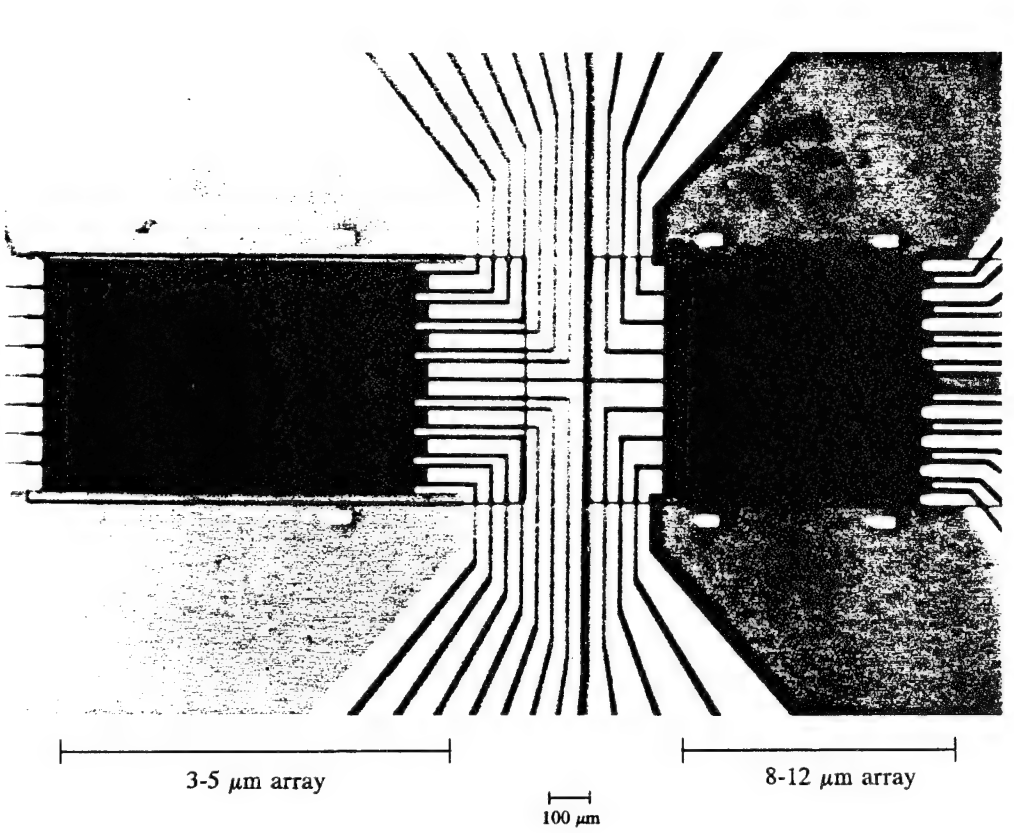

Fig. 8. Dual waveband FLIR detector.

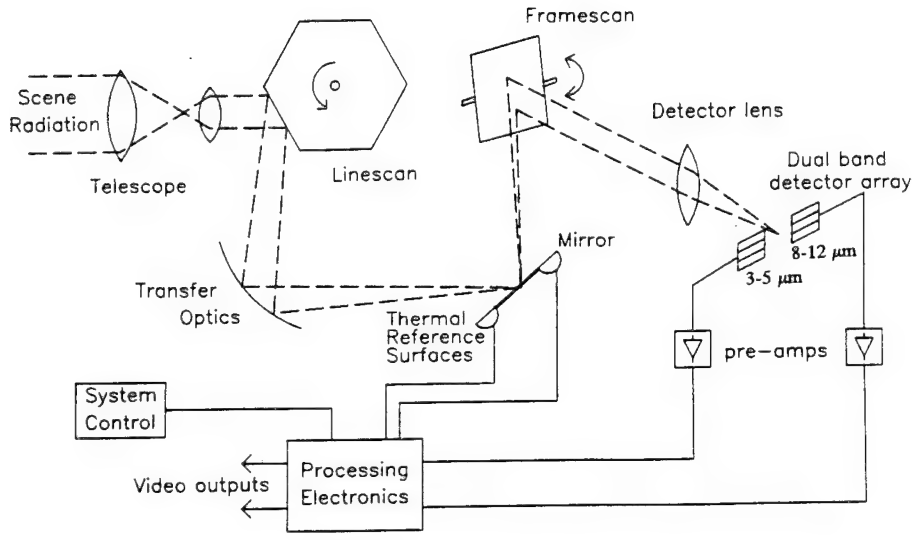

Fig. 9. FLIR operational scheme.[2]

FLIR MEASUREMENT

To effectively calibrate the FLIR, a rudimentary theory must be constructed that includes the FLIR measurement as well as its errors. Measurements must then be carried out to test the theory and to assign magnitudes to the errors. If the errors given by theory and experiment are about the same magnitude and follow similar trends as a function of experimental variables, the errors may be considered as being reasonably well understood and accounted for.

Fortunately, a very good theory in first approximation has been constructed for the FLIR by Braim.[2] In his treatment, the FLIR is assumed to view a large target which radiates in accordance with Planck's blackbody formula:

$$W(T) = \frac{C_1}{\lambda^5[\exp(C_2/\lambda T)-1]} \tag{1}$$

where:

W	=	emitted flux, $W/m^2/\mu m$
T	=	absolute temperature, K
λ	=	wavelength, μm
C_1	=	3.7415×10^8, μm^2
C_2	=	1.4388×10^4, μm K

The FLIR detector produces a signal voltage, S, which depends upon the received flux, ϕ, according to

$$S=\int R\phi d\lambda \tag{2}$$

where R is the detector responsivity. The flux that reaches the detector from the target has contributions from all components in the optical path originating at the target, t. These components are: the atmosphere, a; the magnification optics, o; and the FLIR scanner, s. Each of these components is assumed to have an emissivity

$$\epsilon=\alpha \ , \tag{3}$$

where α is the component absorptivity. If for each component,

$$\alpha+\tau=1 \ , \tag{4}$$

where τ is the component transmissivity, then

$$\epsilon = 1 - \tau \quad . \tag{5}$$

If this expression holds for the emissivity of each component, then the flux generated by each component along the optical path is

$$\phi_a = W(T_t)\tau_a + W(T_a)(1-\tau_a) \quad , \tag{6}$$

$$\phi_0 = \phi_a \tau_0 + W(T_0)(1-\tau_a) \quad , \tag{7}$$

$$\phi_s = \phi_0 \tau_s + W(T_s)(1-\tau_s) \quad . \tag{8}$$

Insertion of these component contributions to the flux into Eq. (2) results in a signal voltage at the detector due to the target

$$\begin{aligned} S_t = & \int RW(T_t)\tau_a\tau_0\tau_s d\lambda + \int RW(T_a)(1-\tau_a)\tau_0\tau_s d\lambda \\ & + \int RW(T_0)(1-\tau_0)\tau_s d\lambda + \int RW(T_s)(1-\tau_s) d\lambda \end{aligned} \tag{9}$$

In this equation the four integrals on the right hand side represent emission from the target, the atmosphere, the magnification optics, and the scanner, respectively. The flux that reaches the detector from the internal reference surface contains contributions from the components in the optical path originating at the reference surface. In this case the only such component is the FLIR scanner. Beyond this component, the flux is

$$\phi_s = W(T_{ref}) + W(T_s)(1-\tau_s) \quad . \tag{10}$$

Inserting this expression into Eq. (2) yields the signal voltage at the detector due to the reference surface

$$S_{ref} = \int RW(T_{ref})\tau_s d\lambda + \int RW(T_s)(1-\tau_s) d\lambda \quad . \tag{11}$$

The two integrals on the right-hand side of Eq. (11) represent the emission from the reference surface and from the scanner, respectively. A temperature reading given by a platinum wire resistance in contact with a reference surface is obtained by adjusting the Peltier device of the surface so that the gray scale response of the target and reference surface match. Thus,

$$S_t = S_{ref} \quad . \tag{12}$$

Rearranging slightly and using Eqs. (9) and (11)

$$\int RW(T_t)\tau_a\tau_0\tau_s d\lambda = \int RW(T_{ref})\tau_s d\lambda - \int RW(T_a)(1-\tau_a)\tau_0\tau_s d\lambda - \int RW(T_0)(1-\tau_0)\tau_s d\lambda \tag{13}$$

Note that under conditions of the same gray scale response from target and internal reference surface, the emission from the target is equal to that from the reference surface reduced by contributions from the atmosphere and the magnification optics. In case Eq. (12) holds, there is no contribution due to scanner emission.

Equation (13) may be used for FLIR calibration. Imagine for simplicity an ideal case whereby

$$\tau_a = \tau_0 = 1 \quad . \tag{14}$$

In this case, Eq. (13) reduces to

$$\int RW(T_t)\tau_s d\lambda = \int RW(T_{ref})\tau_s d\lambda \quad . \tag{15}$$

Thus, if the atmosphere and optical train do not result in any detectable emissions, matching the gray scale responses of target and reference surface also matches their respective temperatures. This is a case where it is conceptually simple to calibrate T_{ref}. For a range of target temperatures T_t, the reference surface Peltier device is adjusted so that target and reference surfaces both have the same gray scale responses. Then $T_t = T_{ref}$.

On the other hand, if

$$\tau_a = 1 \quad , \tag{16}$$

then Eq. (13) reduces to

$$\int RW(T_t)\tau_0\tau_s d\lambda = \int RW(T_{ref})\tau_s d\lambda - \int RW(T_0)(1-\tau_0)\tau_s d\lambda \tag{17}$$

The last integral on the right-hand side of Eq. (17) represents a correction term to the first integral on the same side; that is, it plays the role of a systematic error. Matching the gray scale response of target and reference surface no longer implies that $T_t = T_{ref}$, as was the case previously. Although this would still be approximately true, the actual temperature T_{ref}, for given values of T_t and T_o, can be obtained by using an iterative solution to Eq. (17).

Different values of T_o will modify the solution obtained for T_{ref}, signifying that the temperature of the magnification optics introduces a systematic error into the determination of T_{ref} by the process of requiring Eq. (12) to hold. The magnitude of that systematic error is controlled by the last integral in Eq. (17). As the transmissivity of the optical train τ_o approaches unity (that is, as the emissivity vanishes), so too does the systematic error, and Eq. (17) reverts back to Eq. (15).

Considering Eq. (13) in light of these last remarks, it appears that the integrals subtracted on the right-hand side describe the atmospheric emission and the optical emission, respectively. These are the systematic errors due to temperature matching of the gray scale response of the target and the internal reference surface, respectively. To show in a quantitative manner that Eq. (13) represents a valid description of the temperature measurement and its errors, requires that the quantities in question be both calculated and measured. Braim has done that for the 8- to 12-μm waveband; see Fig. 10. Figure 10a shows the experimentally measured results of T_{ref} versus T_t, for a variety of different temperatures, T_o of the optical train. Note that with increasing T_o, T_{ref} is forced to increase to compensate for the effect of increased radiation from the optical train, in accordance with Eq. (13). Part (B) of the figure presents theoretically calculated results, based on Eq. (13), of T_{ref} versus T_t, for a variety of different optical train temperatures, T_o. A clear correlation exists between the experimental and theoretical results, which lends confidence to Eq. (13) as a good first-order description of the FLIR temperature measurement and its errors.

Although the full calibration described by Eq. (13) takes into account the atmospheric transmissivity, τ_a, and temperature, T_a, these quantities are not considered in Fig. 10. This is a matter of first-order expediency, and a more complete treatment should also take into account systematic errors due to the atmosphere.

Greater understanding of the FLIR calibration process has been gained through measurement of T_{ref}. The FLIR produces a gray scale response to a blackbody target with known temperature which is considered to be a standard value. The temperature of the Peltier internal reference surface is adjusted so that its gray scale response matches the standard, a condition that is embodied in Eq. (13). The resistance measurement of the temperature, T_{ref}, of the internal reference via a platinum wire resistance, is correlated to the blackbody target temperature, T_t. This correlation is established over a temperature range of interest for a fixed value of the magnification optical components temperature, T_o. In order to remove the systematic error associated with the optical train temperature, T_o, in Eq. (13), T_{ref} versus T_t is measured for a range of temperatures, T_o, building a set of experimental calibration curves similar to those displayed in Fig. 10a. Such curves allow the measurement of an unknown apparent temperature, T_t, of a target by means of

matching the internal reference temperature gray scale responses. It may thus be possible to remove the systematic error due to T_o.

Calibration of the internal reference surface temperature, T_{ref}, is adequate for measuring the temperature, T_t, of an extended target with uniform temperature. Many targets of interest are characterized by a nonuniform temperature distribution, which corresponds to a number of different gray scale responses. This case requires the calibration of the entire gray scale for every pixel of an image frame. The following gray scale calibration is based upon the calibration of both internal reference surfaces using the method already presented.

GRAY SCALE CALIBRATION BY LINEAR INTERPOLATION

Assume that the temperatures of the two internal reference surfaces are calibrated using the theory shown in Fig. 10 and consistent with Eq. (13). For each discrete temperature of a reference surface there is a corresponding gray scale response curve. For each set of reference surface temperatures there is a corresponding gray scale response curve. The desire is therefore for an interpolation scheme that assigns temperatures to the gray scale data of a given image frame.

Assuming that the gray scale response, G, is a function of temperature, T, which to first-order may be expanded by a Taylor-series of the form

$$G(T) = G(T_1)+(T-T_1)\frac{\delta G(T_1)}{\delta T} , \tag{18}$$

where T_1 and T_2 are the temperatures of the two reference surfaces. A finite difference evaluation of the first derivative of Eq. (18) produces

$$\frac{\delta G(T_1)}{\delta T} = \frac{G(T_2)-G(T_1)}{T_2-T_1} . \tag{19}$$

The Taylor-series expansion becomes

$$G(T)=G(T_1)+(T-T_1)\ \frac{G(T_2)-G(T_1)}{T_2-T_1} , \tag{20}$$

which, if solved for T, yields

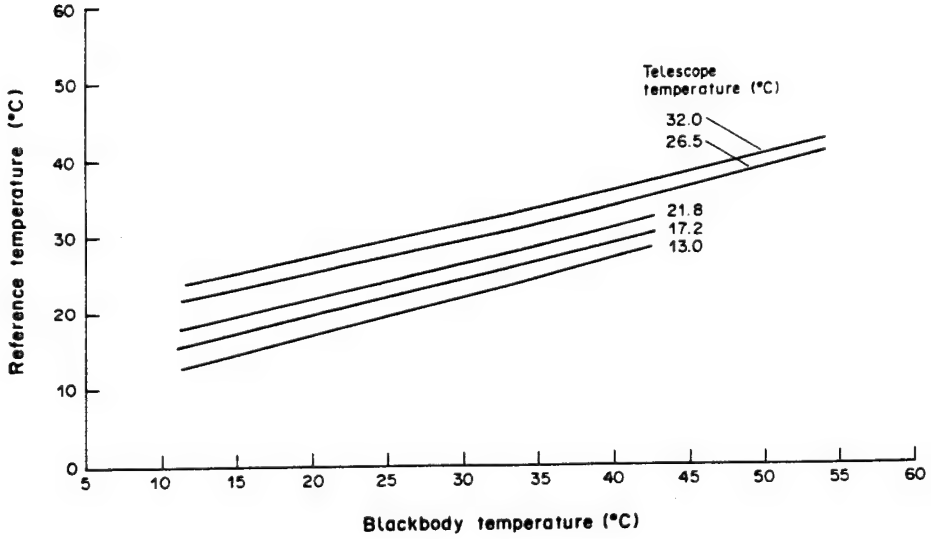

Fig. 10a. Experimental measurements.

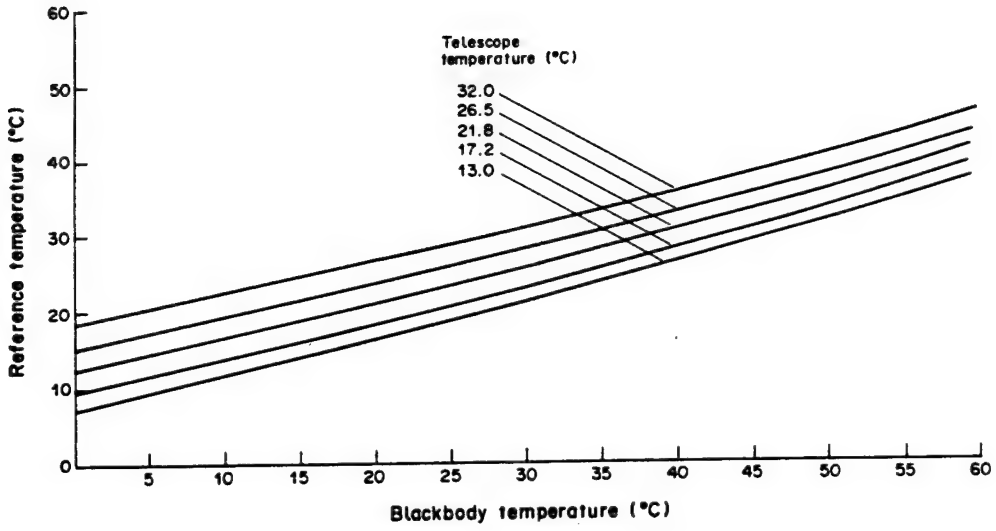

Fig. 10b. Corresponding theoretical results.

Fig. 10. Internal reference surface temperature calibration of Braim.[2]

$$T=T_1+[G(T)-G(T_1)]\ \frac{(T_2-T_1)}{[G(T_2)-G(T_1)]}\ . \tag{21}$$

Defining

$$\Delta T=[G(T)-G(T_1)]\ \frac{(T_2-T_1)}{[G(T_2)-G(T_1)]} \tag{22}$$

obtains

$$T=T_1+\Delta T\ . \tag{23}$$

The gray scale response, G, of a given pixel in an image may thus be used to obtain the temperature, T, of that same pixel.

Since the Planck blackbody curve is not linear in temperature, a linear interpolation scheme will increasingly become more unreliable as the separation of the two reference temperatures, T_2 and T_1, increases. The magnitude of the error due to linear interpolation may be estimated by calculating the signal voltage

$$S_i=\int RW(T_q)d\lambda \qquad i=1,2 \tag{24}$$

at the two reference temperatures, and then taking the "midpoint" signal

$$\bar{S}=\frac{1}{2}(S_1+S_2)\ , \tag{25}$$

which occurs at the midpoint temperature

$$\bar{T}=\frac{1}{2}(T_1+T_2)\ . \tag{26}$$

$\bar{S}$ may be obtained through the use of a relationship between the signal voltage and the temperature, such as Eq. (24). The results of the calculations performed in this manner by Braim are shown in Fig. 11. The error due to linear interpolation of the gray scale is seen to increase with the temperature interval, T_2 - T_1, and can easily amount to a few degrees absolute. In the shorter waveband, the corresponding errors are noticeably larger.

GRAY SCALE CALIBRATION BY NONLINEAR INTERPOLATION

The use of a linear interpolation scheme introduces an extraneous systematic error into the final result. More data exist in the gray scale than are used by a linear interpolation method. A linear interpolation scheme establishes a linear relationship between the signal received by the detector from an element of the target and the temperature of that target element. The detector responds to radiation described by the Planck blackbody expression which is not linear in T. Thus a systematic error is introduced by the linear interpolation scheme. This systematic error can be eliminated or reduced through the use of nonlinear interpolation.

The platinum resistance temperature reading of an internal reference surface, of course, is independent of the changing electronic "window" and "offset" values. The reference surface temperatures are thus calibrated against a blackbody reference source. Given such a calibration, the task now is to use that information to calibrate the gray scale without introducing the systematic error associated with a linear interpolation.

The gray scale response of a reference surface ideally is linear in the signal voltage induced in the detector by radiation from a surface; that is,

$$G(T_1)=k\int R[W(T_1)+W(T_s)(1-\tau_s)]d\lambda \quad , \tag{27}$$

where k is a proportionality constant, the magnitude of which is fixed by the amplification electronics of the FLIR, W is the Planck blackbody function, R is the response function of the detector, T_1 is a reference surface temperature, and T_s is the temperature of the scanner. The constant satisfies

$$k = k(W,O) \quad , \tag{28}$$

that is, the constant is a function of the electronic "window" W and "offset" O parameters. This makes the gray scale response inconvenient to calibrate directly against a blackbody source. For any given frame of image data the constant k may be evaluated from Eq. (27). Thus,

$$k(W,O)=\frac{G(T_1)}{\int R[W(T_1)+W(T_S)(1-\tau_S)]d\lambda} \quad . \tag{29}$$

Such determination of k requires that the detector responsivity and the scanner transmissivity have been measured. From the Eq. (29), the value of k can be used to solve for the temperature, T, to be assigned to every pixel in the image frame. For any pixel the gray scale response is

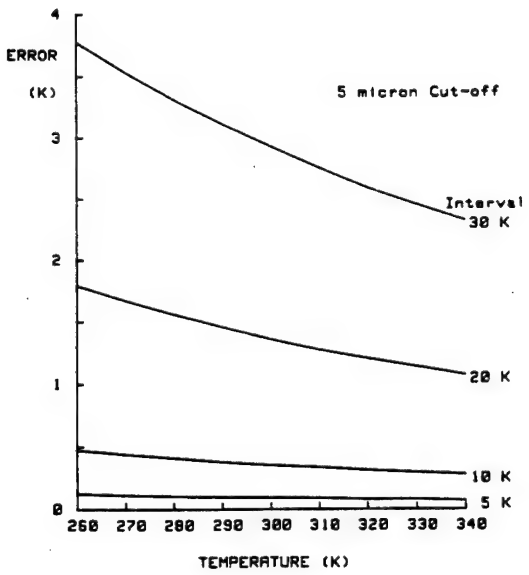

Fig. 11a. 5-μm wide spectral window.

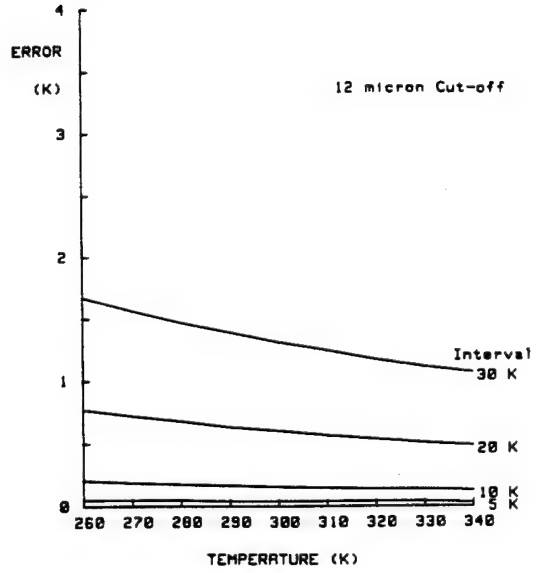

Fig. 11b. 12-μm wide spectral window.

Fig. 11. Estimated errors in target apparent temperature due to linear interpolation.[2]

$$G(T)=k\int R[W(T)+W(T_S)(1-\tau_S)]d\lambda \quad . \tag{30}$$

This equation may be solved iteratively for the temperature of the pixel, circumventing any linear interpolation scheme.

An iterative solution to this equation may be considered somewhat inconvenient. In which case, an interpolation scheme, which include the information contained in the constant k and given by Eq. (29), would be somewhat superior to a linear one.

Instead of using Eq. (30) to solve for all the values of T and all pixel values G, it is used only once to solve for G corresponding to a T value half way between two reference surface temperatures, T_1 and T_2. Thus,

$$T_h=T_1+h \tag{31}$$

where

$$h = \frac{1}{2}(T_2-T_1) \tag{32}$$

If one Taylor-expands the gray scale response, G, to second-order,

$$G(T)=T(T_1)+(T-T_1)\frac{\delta G(T_1)}{\delta T}+\frac{(T-T_1)^2}{2}\frac{\delta^2 G(T_1)}{\delta T^2} \quad . \tag{33}$$

Inserting T_h into Eq. (30) results in G for three temperatures, T_1, T_h, and T_2. Knowledge of G at three temperatures allows an evaluation of both the first and second derivatives by finite difference approximations given by

$$\frac{\delta G}{\delta T}(T_1) = \frac{G(T_1+h)-G(T_1)}{h} \tag{34}$$

and

$$\frac{\delta^2 G(T_1)}{\delta T^2} = \frac{G(T_1+2h) - 2G(T_1+h)+G(T_1)}{h^2} \quad , \tag{35}$$

respectively.

If the gray scale response, G, is Taylor-series expanded to second-order, then

$$G(T) = G(T_1)+(T-T_1)\frac{\delta G(T_1)}{\delta T}+\frac{(T-T_1)^2}{2}\frac{\delta^2 G(T_1)}{\delta T^2} \tag{36}$$

using

$$\Delta T=(T-T_1) \ . \tag{37}$$

The Taylor-series expansion is a quadratic equation in the variable ΔT; that is,

$$(\Delta T)^2\left[\frac{1}{2}\frac{\delta^2 G}{\delta T}(T_1)\right]+\Delta T\left[\frac{\delta G(T_1)}{\delta T}\right]+[G(T_1)-G(T)]=0 \tag{38}$$

with solution

$$\Delta T=\frac{\frac{-\delta G}{\delta T}(T_1)\pm\left\{\left[\frac{\delta G}{\delta T}(T_1)\right]^2-4\left[\frac{1}{2}\frac{\delta^2 G(T_1)}{\delta T^2}\right]\left[G(T_1)-G(T)\right]\right\}^{1/2}}{\frac{\delta^2 G(T_1)}{\delta T^2}} \ . \tag{39}$$

Using Eq. (39), the temperature of any pixel with gray scale response G(T), becomes

$$T=T_1+\Delta T \ . \tag{40}$$

Equation (40) is a nonlinear interpolation formula valid to second-order in the Taylor-series expansion of the gray scale response.

Figure 12 indicates qualitatively the nature of the improvement expected when using the nonlinear second-order interpolation formula, Eqs. (39) and (40), instead of the linear first-order interpolation formula, Eqs. (22) and (23). The points in Fig. (12), labeled 1, 2, and 3 refer to a Taylor-series expansion evaluated up to order zero, one, and two, respectively. Examination also indicates two reference data points determine the first derivative of a function and three reference data points determine the second derivative, respectively.

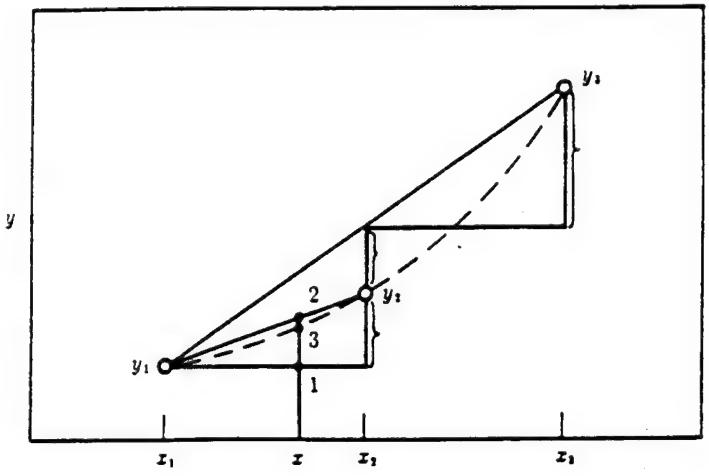

Fig. 12. Comparison of various orders of interpolation.

CONCLUSIONS AND RECOMMENDATIONS

A FLIR can be used as an imaging radiometer for quantifying the infrared contrast between a ship and its background will have qualitative value only if care is taken in the calibration of the instrument.

Following the theory of Braim, the importance of the removal of one systematic measurement error due to emission from the FLIR optical train is explained. Another source of systematic error, attributable to analysis of the FLIR gray scale response and based upon a method of linear interpolation, may be eliminated.

A novel analysis, both nonlinear and iterative, using a second-order Taylor series expansion, is presented. It is believed that this method may, at least, largely reduce the calibration systematic error introduced by the linear interpolation method of calibration.

Further analysis is required to analyze the nature of the random errors associated with FLIR measurements.

THIS PAGE INTENTIONALLY LEFT BLANK

BIBLIOGRAPHY

1. Braim, S.P. and G.M. Cuthbertson, SPIE Vol. 685, Infrared Technology XII, pp. 129-37 (1986).

2. Braim, S.P. "Technique for the Analysis of Data from an Imaging Infrared Radiometer," *Infrared Phys.*, Vol. 28, No. 4, pp. 255-261 (1988).

THIS PAGE INTENTIONALLY LEFT BLANK

INITIAL DISTRIBUTION

Copies			
5	OCNR		
	1	33	A. Tucker
	1	33	J. Gagorik
	1	35	J.L. Gore
	1	35	D. Stegman
	1	35	S. Zakanycz
3	NAVSEA		
	1	03T4	LT W. Brooks
	1	03T4	P. Chatterton
	1	03T4	P. Covich
8	NRL		
	1	5620	J. Kershenstein
	1	5620	M. Mermelstein
	1	5620	R. Priest
	1	5620	K. Snail
	1	5620	E.J. Stone
	1	5750	G. Friedman
	1	5750	P. Mak
	1	5750	S. Moroz
1	Library of Congress Science and Technology Division		
1	USNA/Tech Library		
2	DTIC		

Copies	
1	NASA Scientific and Information Facility
20	CUNY Chemistry Department L. Massa
1	PAR Government Systems Group C. Acquista

DIVISION DISTRIBUTION

Copies	Code	Name
1	0112	B. Douglas
1	3421	TIC (C)
1	3422	TIC (A)
10	3432	Reports Control
1	70′	M. Sevik
1	7010	G. Smith
1	7070	W. Nichols
1	7080	M.A. Sekellick
1	7200	J.H. King
1	7220	P. Hart
1	7220	R. Warfield
1	7220	D. Weiss
1	7220	K. Wilson
1	7220	J. Young
1	7230	W. Bird
20	7230	P. Cervenka
1	7230	D. Etherton
1	7230	S. Kerr
1	7230	P. Ostrowski
1	7230	R. Ratcliffe
1	7230	R. Schwartz
1	7230	R. Snedegar
1	7240	A. Stoyanov
1	7240	Y. Stoyanov
1	7310	J. Grizzard
1	7310	D. Morgan